AUT Journal of Electrical Engineering

AUT J. Elec. Eng., 53(2) (2021) 189-200
DOI: 10.22060/eej.2021.19374.5389

Entropy Based Parameter Estimation of 2D Gaussian Filter for Image Speckle Noise Removal

Z. Hosseini[1], M.R Hassannejad Bibalan[2*]

[1]Department of Biomedical Engineering, Faculty of Electrical Engineering, K. N. Toosi University of Technology, Tehran, Iran.
[2]Department of Electrical Engineering, Imam Khomeini International University, Qazvin, Iran.

ABSTRACT: In this paper, a speckle noise suppression algorithm based on the 2D Gaussian filter is addressed, which employs entropy to estimate the filter's variance effectively. Speckle noise is an inherent characteristic of the coherent imaging systems, which degrades the quality of the resulting images. Gaussian filter is a traditional approach for speckle denoising. However, estimating its optimum variance is still a challenge. Many algorithms have been developed to estimate the optimum variance, but they suffer from the type of noise or a predetermined variance. Our proposed method demonstrates an improved 2D Gaussian filter since it estimates the optimum variance of the filter in the context of differential entropy between the noisy and filtered images under different p-norms. This optimum variance is directly estimated from the speckle noise level of image and it differs for different types of noise and images. The optimization problem is numerically solved, and the value of the norm order is also appropriately determined. The blind estimation of norm order is also accomplished based on the level of noise variance. Finally, the proposed method's performance is appraised, utilizing both standard and real ultrasound (US) images. The quality of filtered images is assessed through the qualitative and quantitative simulations in terms of peak signal to noise ratio (PSNR), correlation coefficient (CoC), structural similarity (SSIM), and equivalent number of looks (ENL). The experimental results reveal the proposed method's proficiency in contradiction to state-of-the-art despeckling methods through the capability of strong speckle noise removal and preserving the edges and local features.

Review History:
Received: Dec. 12, 2020
Revised: Dec. 03, 2021
Accepted: Mar. 13, 2021
Available Online: Sep. 01, 2021

Keywords:
Image Denoising
2D Gaussian Filter
Speckle Noise
Entropy

1- INTRODUCTION

US imaging is a non-invasive imaging modality that captures images of the internal organs of the human body [1]. This medical imaging system has enormous medical field applications such as diagnosis, check-ups, and guidance tools in surgeries due to its real-time, portable, affordable, and non-ionizing capabilities [2]. However, its images suffer from artifacts, low resolution, and contrast [3]. The main reason for the declined quality of US images is the speckle noise resulting from the constructive and destructive interference of backscattered echo signals [4]. The speckled image might lead to a wrong decision of physicians [5, 6]. Thus, the speckle noise suppression from US images is of great importance in medical image processing. Some basic descriptions of image, noise, and several common speckle noise removal methods are given in the following.

The visual depiction of real objects is image. During the process of transmission or acquisition of images, a granular pattern is introduced, which creates problems for further operations [7]. The phenomenon that makes the image appearance grainy is called noise. Noise is a random variation in image intensities, which makes the image interpretation challenging [8]. From the noise source point of view, two primary multiplicative and additive noise models have been introduced [9]. Suppressing the additive noise is easy due to its systematic nature, the ability of easy modeling, and the feature of signal Independence [10]. On the other hand, multiplicative noise has complex modeling features making multiplicative noise reduction problematic. In particular US, Speckle is a multiplicative noise that appears in coherent imaging systems, laser, and airborne remote sensing [11, 12]. This type of noise is responsible for the granularity [13, 14] and poor visibility by decreasing the contrast of essential details and resolution, which plays a critical role in segmentation and edge detection [15, 16]. Speckle removal or despeckling facilitates subsequent analysis of the image and improves the quality metrics [17].

Numerous studies have been conducted to effectively suppress the speckle noise while retaining the images' vital details. Despeckling filters proposed in these studies can be classified into spatial, wavelet-based and nonlocal mean filters [18]. Median [19], Wiener [20], neighbor pixels averaging (NPA) [21], Lee [22], and Kuan [23] are the most efficient spatial filters. They perform well in image despeckling. However, they cannot differentiate between the edges and noise existing in the image, which is the main limitation of these filters resulting in blurring the edges [24].

*Corresponding author's email: mhbibalan@ieee.org

Wavelet-based denoising methods are the second class of despeckling filters. Despite being successful in preserving image resolution, ringing effects close to the edges show that more developments are required to make this filtering class universally effective [17, 25]. The last is Nonlocal mean filters, which can preserve edges efficiently [26, 27]. The main drawback of this category is their blurring and adhesive effects on images.

Gaussian filter is an example of spatial filters which is capable of proficiency restoring the grainy image [25]. Due to various types of edges and noise levels in each part of the image, it is essential to apply different degrees of smoothness provided by the Gaussian filter. Hence, this paper's main contribution is to present an improved 2D Gaussian filter with an optimal variance using the entropy concept to suppress the speckle noise efficiently. To this end, the p -norm between the noisy and denoised images is calculated. Afterward, the entropy of the calculated p -norm is determined. Moreover, the optimal variance is obtained by identifying the point with the highest slop tangent line corresponding to the differential entropy function. The estimation of p in two cases of having or not having an estimate of noise variance is discussed.

The remainder of this paper is structured as follows. Section 2 presents the speckle noise model in US images. In section 3, 2D Gaussian filtering and a brief review of well-known Gaussian methods are given. Our novel despeckling strategy is covered in section 4. In Section 5, the proposed method's performance analysis is appraised compared to the state-of-the-art speckle noise reduction methods. Finally, the paper is concluded in section 6.

2- SPECKLE NOISE MODEL IN US IMAGES

In this section, a brief explanation of the speckle noise model in US Images is provided. Let us consider an image acquired by the US scanner. This image contains speckle noise, which affects the human interpretation to differentiate the fine details by its granular pattern. The approximate general Two-dimensional model of US image influenced by speckle noise is represented as [28]:

$$I(x,y) = f(x,y)\eta(x,y) + \nu(x,y), \tag{1}$$

where $I(x,y)$ is the degraded image by the multiplicative and additive noises, $f(x,y)$ denotes the noise-free image and $\eta(x,y)$ and $\nu(x,y)$ are the speckle and additive noise components. In this equation, x and y depict the axial and lateral pixel position. Due to the less importance of the additive component in contradiction to the multiplicative component, Eq. (1) can be rewritten as [28]:

$$I(x,y) = f(x,y)\eta(x,y). \tag{2}$$

Such models help us smooth the uniform regions of image where the signal is approximately supposed to be constant. In US imaging systems, echo signals need to be compressed to be displayed on a monitor. The compression can be applied using a log transformation. Log transformation not only converts the multiplicative noise to an additive one but also leads to amplify powerless backscatters [20]. Moreover, it simplifies the US image filtration since the speckle noise is considered as white additive Gaussian noise after the transformation. By applying a log-transformation on both sides of Eq. (2), the following equation is obtained [20]:

$$\ln I(x,y) = \ln f(x,y) + \ln \eta(x,y). \tag{3}$$

In this equation, the $\eta(x,y)$ is approximately the white Gaussian noise.

3- SPECKLE REMOVAL USING GAUSSIAN FILTER

Gaussian filter is a linear approach that is extensively utilized as a low pass filter to remove different kinds of noise. As stated in [25], we employ a 2D Gaussian filter as follows:

$$G(x,y;\sigma) = \frac{1}{2\pi\sigma^2} e^{-\frac{x^2+y^2}{2\sigma^2}}, \tag{4}$$

where σ^2 represents the variance and determines the shape of the filter. In order to assess the smoothing effect of σ^2, a 2D Gaussian filter is applied on Pirate image with different values of σ^2. The results are shown in Fig. 1. Fig. 1(a,b) represent the 2D Gaussian filter shape with $\sigma^2 = 2$ and 5. Additionally, the corresponding filtered images are exhibited in Fig. 1(c,d). It is clear that as the amount of σ^2 increases, the amount of smoothing, and image details such as edges enhance and the borders become more blurred.

Filtering by a 2D Gaussian filter can be viewed as a convolution taken based on the 2D Gaussian kernel. In other words, the center pixel of the kernel will be replaced by the weighted averaging of its own and neighbors' pixels where the weighing factors follow from Eq. (4). Such an operation will be continued by sliding the window through all the image pixels.

It is noteworthy to mention that determining the variance value has been a high priority issue in the last decades. One of the initial works on the image noise reduction issue using an optimal Gaussian filter can be traced back to [29] when the authors demonstrate a relationship between noise statistics knowledge and choosing an optimum Gaussian filter. Initially, they depict that the Gaussian filter's properties associate with the noise statistics and the signal. Afterwards, according to the derived relationship, an optimal Gaussian filter is identified that is able to suppress the noise efficiently. Another study proposed an adaptive noise removal method in which the strength changes based on the noise type, image contrast, and the intensity [25]. The proposed method is made up of a Gaussian core with a variable kernel structure. Likewise, to achieve efficient denoising results, the smoothing strength is supervised by a neural network. In [30]. the author recommended a novel variance estimator for the Gaussian

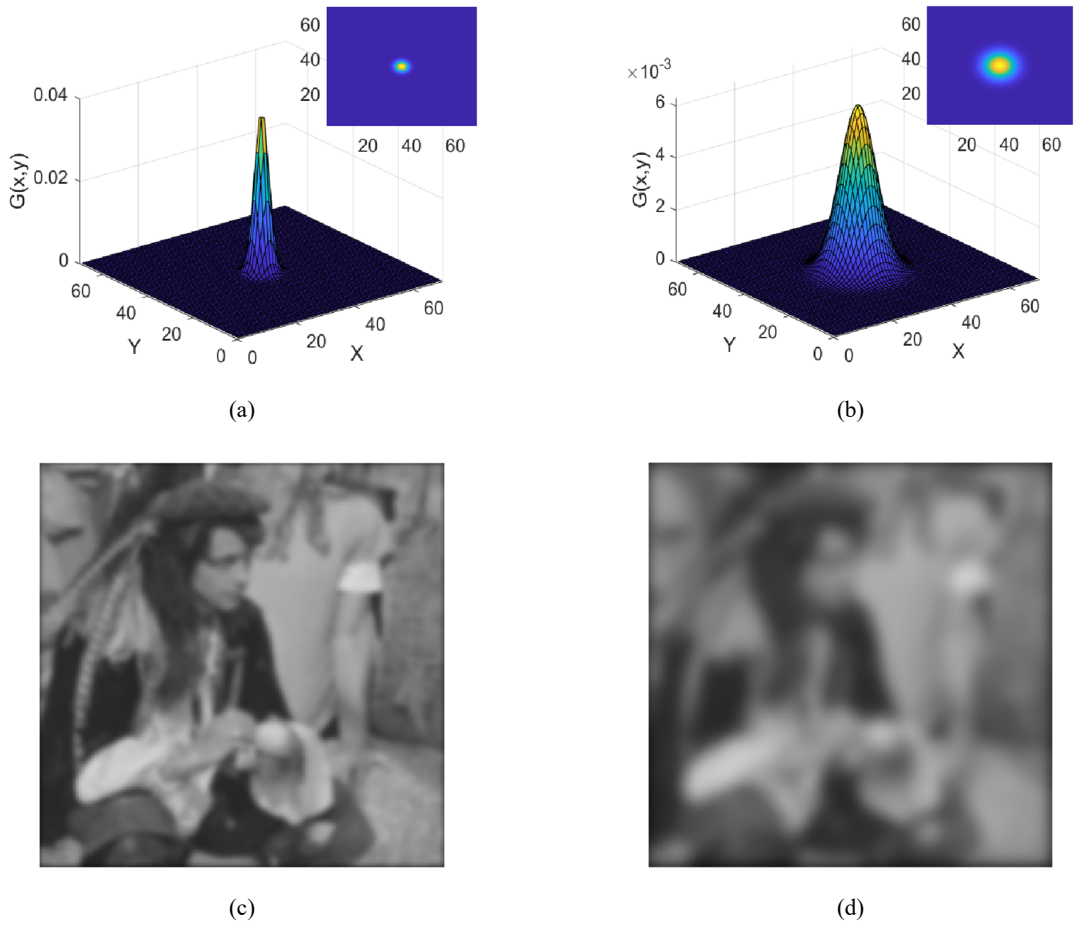

(a) (b)

(c) (d)

Fig. 1. Performance comparison of the 2D Gaussian filter in terms of different σ values. (a, b) 2D Gaussian filter shape with σ=2 and 5. (c, d) Corresponding filtered images.

filter to denoise the image based on the relationship between the linear diffusion and Gaussian scale space. In such studies, the image gradient's median absolute and the noise variance are utilized to match the estimates to the image structure. The results indicate that such an adaptive Gaussian filter has superior results compared to noise diffusion filters. Another attempt in image denoising domain is [31], in which a new methodology to estimate the variance value of the Gaussian filter is developed. In this work, an adaptive Gaussian filtering algorithm based on Hudson's work is introduced. Additionally, the filter's variance is adapted to the signal's local variance and noise characteristics. Images filtered by such a Gaussian method have smaller mean square errors than those filtered by non-adaptive Gaussian techniques. Furthermore, the edge points will be less distorted by the adaptive Gaussian filter, since the filter's variance have the minimum values there.

Despite all its advantages, there is an assumption constraining the application of the mentioned filter, which is the image's noise type that should be Gaussian noise with a known variance.

Different kinds of images have different types of histograms and intensities. By considering the effect of noise and their various variance, applying a Gaussian filter with a predetermined variance will not give an admissible outcome. Meanwhile, the determination of variance of the Gaussian filter should be according to the image content. In this paper, we are determined to introduce an approved 2D Gaussian filter with changeable variance regarding the image content.

4- PROPOSED METHOD

Now, we propose an improved 2D Gaussian filter which reduces the speckle noise effectually. To achieve this goal, the noise removal equation of the noisy image using a 2D Gaussian filter is presented as the following:

$$\hat{I}(x,y;\sigma) = I(x,y) * G(x,y;\sigma) = \frac{1}{2\pi\sigma^2}\int_{\alpha}\int_{\beta} I(\alpha,\beta)\, e^{-\frac{(x-\alpha)^2+(y-\beta)^2}{2\sigma^2}}\, d\beta d\alpha, \quad (5)$$

where $\hat{I}(x,y;\sigma)$ shows the filtered or denoised image and $*$ denotes convolution operator. To improve the performance, a variance value estimation for the 2D Gaussian filter is discussed. We aim to estimate the variance based on the p

-norm distance of the noisy image and the filtered one. Its mathematical representation is expressed as:

$$D\left(I,\hat{I};\sigma\right)=\left|I\left(x,y\right)-\hat{I}\left(x,y;\sigma\right)\right|^{p}, \tag{6}$$

where $p>1$ is the norm order and D denotes a measure of the difference between the two images. Afterwards, we need to appropriately determine the value of σ, which ensures the optimum filtering in the context of distance mentioned before. Moreover, the original noise-free image is not accessible. Many techniques use a predefined constant value for σ to overcome this problem. We introduce an approach based on the entropy concept to obtain the optimum σ. Entropy is a statistical measure of randomness. Recently, the entropy concept has been extensively applied on image segmentation [32] and optoacoustic tomographic image reconstruction [33]. In this work, we utilize entropy in the content of Gaussian filter variance estimation to eliminate the speckle noise. To this end, we calculated the entropy of Eq. (6) as follows:

$$H_{D}\left(I,\hat{I};\sigma\right)=-\int_{x}\int_{y}p_{D}\left(x,y\right)\ln p_{D}\left(x,y\right)dydx, \tag{7}$$

where $p_{D}\left(x,y\right)$ is the probability density function of $D\left(I,\hat{I};\sigma\right)$. In order to find the optimum σ, we have defined an optimization problem on the entropy using 500 points in the interval of 0 to 5. A typical diagram of obtained entropy is illustrated in Fig. 2(a). This figure shows that as the value of standard deviation (std) increases, the differential entropy's behavior increases monotonically. Thus, we are looking for a point where the tangent line has the highest slope to the differential entropy curve. Such point corresponds to the optimum std (variance). The proposed method considers the optimum value of σ as the point where the entropy derivative has its maximum value. To find the optimal variance, the derivative of obtained entropy curve is computed. The derivative function of Eq. (7) and its maximum value are also plotted in Fig. 2(b). The maximum value for the derivative of differential entropy corresponds to the differential entropy curve's tangent line with the max slope. Finally, the optimal std value is calculated as:

$$\hat{\sigma}=\sqrt[p]{\arg\max_{\sigma}\frac{d}{d\sigma}H_{D}\left(I,\hat{I};\sigma\right)}. \tag{8}$$

According to this relation, the effect of the norm order (p) has been taken into account in the computation of the optimal σ. As the last step, the appropriate norm order must be introduced simply and comprehensively.

5- NORM ORDER ESTIMATION

Choosing the proper p plays a vital role in parameter estimation of 2D Gaussian filter based on the addressed technique. The selection procedure is categorized into two cases, having or not having an estimate of the variance of speckle noise.

In the case of having a noise variance estimation, we introduced a relationship between p and the noise variance. We used regression to estimate the value of p. It was observed according to the made efforts that the p value varies linearly with the noise variance. Hence, we performed a two order linear regression on std. Afterwards, we could find its coefficients according to the optimization and rounding made. Thus, the approximate estimation of p behavior versus the different values of speckle variance is as follows:

$$p=40\sigma_{\eta}^{2}+1, \tag{9}$$

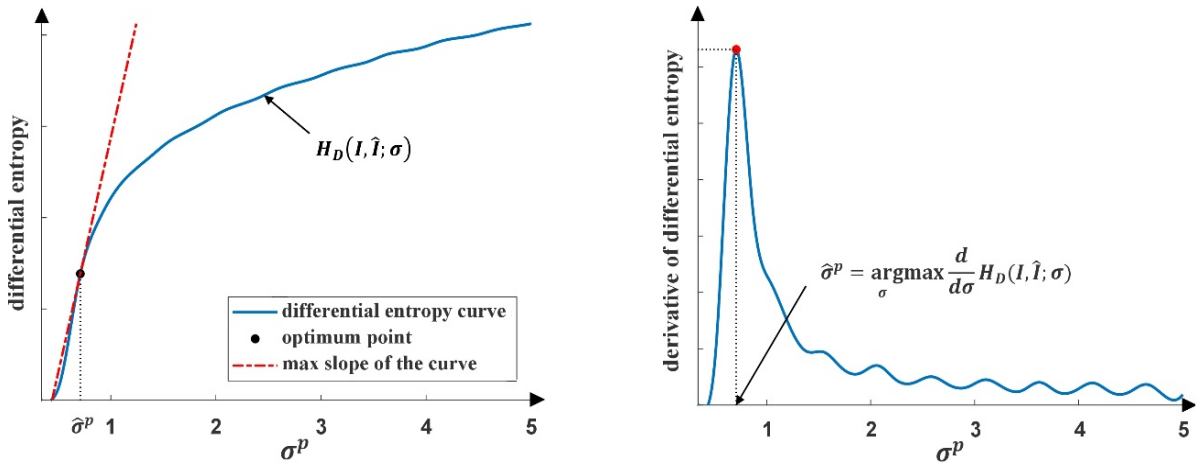

(a) (b)

Fig. 2. Differential entropy curves. (a) p-norm differential entropy curve between noisy and denoised images. (b) Differential entropy derivative curve.

(a) boats (b) cat (c) houses (d) Lena (e) room (f) pirate

Fig. 3. Standard images with resolution of 256×256 pixels

where $0<\sigma_\eta^2<1$ is the normalized speckle noise variance. In introducing the above relation, we have some observations in simulations. For images corrupted by low-level noise, $p=1$ reveals good results. Moreover, by increasing the noise level, p tends to grow to 4, 5, and higher levels for better performance. Based on linear regression, we concluded our observations by fitting a linear curve expressed in Eq. (9).

On the other hand, in the blind case where we have no estimate of the noise variance from the noise level of images, a proper value for p is chosen. Meanwhile, we defined three categories based on the noise level. The first class belongs to high SNR images meaning that they are corrupted by low-level noise. For such an image, the p value is chosen from the range of 1 to 2. The second images are those which are degraded by the medium noise level. For these images, p lies in the interval of 2 to 4. Finally, for the low SNR

images, p takes values greater than 4. The above mentioned p selection procedure is summarized as:

$$\begin{cases}\text{High SNR:} & 1\le p<2\\ \text{Medium SNR:} & 2\le p<4\\ \text{Low SNR:} & 4\le p\end{cases} \tag{10}$$

Our suggestion for the p value per each interval is as follows: if the image has a low-level noise, a good choice can be 1.5. On the other hand, it is better for images with medium-level noise to select the p value as 3 or 4. Finally, the p value of 5 or 6 can be applied for images having a high-level noise.

6- EXPERIMENTAL RESULTS

In this section, an experimental assessment of the proposed method in contradiction to some state-of-the-art despeckling techniques is accomplished.

6-1- Experiments on Standard Images

In this paper, the standard dataset contains six images with a resolution of 256×256 pixels; 1) boats, 2) cat, 3) houses, 4) Lena, 5) room, and 6) pirate as demonstrated in Fig. 3. The noise variance is considered 0.01,

0.05, and 0.1 for low, medium, and high noise levels, respectively. The performance of the proposed method is examined with eight well-known filters: 1) average filter, 2) Wiener filter, 3) adaptive median filter (AMF), 4) Lee filter, 5) Kuan filter, 6) Frost filter, 7) non-local mean (NLM) filter, and 8) wavelet filter. In this paper, the Stein's unbiased risk estimate (SURE), which is one of the more popular selections in the wavelet domain, is used for image denoising. This threshold selection algorithm uses shrinkage operators (soft thresholding) and minimizes a risk function. Additionally, the wavelet filter bank of biorthogonals (bior4.4) is used [34]. Since PSNR, CoC and SSIM are powerful and the most used performance evaluation metrics in the image processing applications, they have been utilized to evaluate the proficiency of the methods [35].

PSNR is one of the image quality evaluation metrics determining the different filtering techniques effects [20]. It is the maximum signal-to-noise ratio and represents the relationship between the original image and the filtered one [36]. PSNR can be defined as following expression [37, 38]:

$$PSNR=20\log_{10}\left(\frac{MAX_I}{\sqrt{MSE}}\right). \tag{11}$$

In this expression, MAX_I represents the max value of the filtered image and the mean squared error (MSE) can be defined as [20]:

$$MSE=\frac{1}{MN}\sum_{x=1}^{M}\sum_{y=1}^{N}[I(x,y)-\hat{I}(x,y)]^2. \tag{12}$$

The higher PSNR value depicts an improvement in noise reduction.

SSIM is another image quality metric that evaluates the similarity between the reference image and the despeckled image [20, 36]. SSIM is mainly designed based on the multiplicative combination of three comparison measurements, luminance, contrast, and structural [39]. It is computed by [36]:

$$SSIM=\frac{\left(2\mu_x\mu_y+C_1\right)\left(2\mathrm{cov}_{x,y}+C_2\right)}{\left(\mu_x^2+\mu_y^2+C_1\right)\left(\sigma_x^2+\sigma_y^2+C_2\right)}. \tag{13}$$

Fig. 4. Despeckling results for houses image. (a-c) Speckled images with noise variances of 0.01, 0.05 and 0.1, respectively. (d-f) Results by Wiener filter. (g-i) Results by proposed method.

In this equation, μ_x and σ_x represent the mean and standard deviation of x. μ_y and σ_y are the mean and standard deviation of y. C_1 and C_2 are constant values. SSIM values varies in the range of [-1,1]. The closer

the SSIM value is to 1, the more the images become similar to the despeckled and reference images, and there is almost no difference between them [40].

CoC is the last used quality metric on the standard images. CoC represents the linear relationship between the restored and the reference images by calculating their pixels' variation accompanying the two images' average. It is given as [41]:

$$CoC = \frac{\sum (I(x,y) - \bar{I}(x,y))(\hat{I}(x,y) - \bar{\hat{I}}(x,y))}{\sqrt{\sum (I(x,y) - \bar{I}(x,y))^2 \sum (\hat{I}(x,y) - \bar{\hat{I}}(x,y))^2}}, \quad (14)$$

where the $\bar{I}(x,y)$ and $\bar{\hat{I}}(x,y)$ are the mean of original and the filtered images. The range of CoC varies from -1 to 1. The coefficients close to 1 indicate the stronger correlation between the images [21].

Table 1. PSNR (dB) performance analysis of standard images for different speckle noise level.

σ_η^2	Images	AMF	Wiener	average	NLM	Frost	Lee	Kuan	wavelet	proposed
0.01	boats	26.09	29.40	26.43	**30.43**	28.05	27.66	25.37	28.90	29.27
	cat	29.48	31.37	29.43	30.03	30.33	29.94	27.90	30.38	**32.23**
	houses	27.57	30.31	27.84	30.19	29.86	29.57	26.31	29.88	**31.02**
	Lena	26.61	30.07	26.74	**30.56**	28.21	27.74	25.19	29.51	29.36
	room	26.61	29.20	26.26	**30.08**	27.84	27.37	25.10	29.25	29.59
	pirate	27.42	30.36	27.52	30.37	29.05	28.66	26.84	29.69	**30.42**
0.05	boats	19.76	24.22	24.29	25.26	25.20	24.97	23.60	23.56	**25.41**
	cat	23.83	25.80	27.75	24.16	28.39	28.09	26.66	23.78	**28.63**
	houses	21.55	25.13	25.68	25.39	26.90	26.74	24.62	25.02	**27.17**
	Lena	20.64	24.60	24.80	25.44	25.68	25.39	23.75	24.53	**25.85**
	room	20.67	24.70	24.56	25.14	25.58	25.25	23.77	24.84	**25.88**
	pirate	21.27	25.04	25.58	25.39	26.50	26.24	25.12	24.22	**26.69**
0.1	boats	17.08	21.59	22.64	22.92	23.19	23.07	22.17	21.23	**23.76**
	cat	21.22	22.98	26.30	21.75	26.75	26.54	25.52	20.97	**27.10**
	houses	18.83	22.48	23.91	23.38	24.68	24.62	23.19	22.79	**25.28**
	Lena	17.97	22.00	23.21	23.26	23.76	23.60	22.46	22.31	**24.26**
	room	17.97	22.19	23.09	23.15	23.76	23.56	22.49	22.81	**24.27**
	pirate	18.54	22.32	24.00	23.29	24.57	24.43	23.68	21.79	**25.07**

Table 2. SSIM comparison under noise variances of 0.01, 0.05 and 0.1.

σ_η^2	Images	AMF	Wiener	average	NLM	Frost	Lee	Kuan	wavelet	proposed
0.01	boats	0.631	0.801	0.750	**0.823**	0.786	0.777	0.749	0.765	0.778
	cat	0.865	0.887	0.852	0.891	0.871	0.861	0.842	0.901	**0.920**
	houses	0.723	0.820	0.790	0.819	0.821	0.813	0.787	0.807	**0.847**
	Lena	0.642	0.805	0.751	**0.826**	0.790	0.779	0.748	0.792	0.787
	room	0.696	0.815	0.751	**0.845**	0.795	0.780	0.751	0.819	0.832
	pirate	0.735	0.845	0.797	0.843	0.831	0.822	0.800	0.821	**0.853**
0.05	boats	0.399	0.576	0.590	0.598	0.615	0.604	0.589	0.530	**0.629**
	cat	0.694	0.781	0.803	0.754	0.824	0.811	0.794	0.752	**0.836**
	houses	0.454	0.658	0.680	0.648	0.706	0.695	0.678	0.627	**0.723**
	Lena	0.396	0.586	0.601	0.623	0.629	0.617	0.597	0.575	**0.643**
	room	0.431	0.633	0.627	0.638	0.663	0.645	0.627	0.622	**0.683**
	pirate	0.474	0.667	0.683	0.663	0.713	0.701	0.684	0.620	**0.725**
0.1	boats	0.308	0.472	0.506	0.491	0.526	0.515	0.505	0.434	**0.557**
	cat	0.589	0.710	0.758	0.687	0.779	0.765	0.750	0.673	**0.789**
	houses	0.330	0.555	0.596	0.552	0.618	0.606	0.594	0.528	**0.650**
	Lena	0.297	0.476	0.512	0.519	0.535	0.522	0.508	0.472	**0.571**
	room	0.320	0.518	0.540	0.527	0.571	0.553	0.540	0.513	**0.603**
	pirate	0.354	0.562	0.602	0.570	0.627	0.615	0.602	0.518	**0.654**

First, the noise-free images shown in Fig. 3 are degraded with different levels of speckle noise. Afterwards, they are denoised by the techniques mentioned above. Finally, the quantitative results in terms of PSNR, SSIM, and CoC are provided. The merit of the proposed approach is quantitatively and visually assessed on dataset images. It is noted that we used the Monte Carlo method for validation, since the speckle noise is added to the standard dataset and we perform statistical analysis. In other words, for each level of noise, the denoised image is estimated 100 times with different speckle noise and averaged quantitative metrics of these 100 experiments.

To visually assess, our 2D Gaussian filter-based method is compared with the Wiener filter, and the results for the houses image are demonstrated in Fig. 4. This figure shows the three speckled version of the houses image and the corresponding denoised images, using the proposed method and the Wiener filter. Our novel approach reveals a better performance than the Wiener filter, which is one of the most potent filters in preserving fine details and suppressing the speckle noise.

PSNR results provided in Table 1 show the proposed method's noise reduction capability in contradiction to the filters mentioned above. For example, for the Lena image in the case of $\sigma^2 = 0.05$, the proposed filter with a PSNR of

25.85 dB is better, at least with a 0.17 dB margin to the next better one. After the proposed method, the Frost filter has the highest PSNR value of 25.68 dB. Additionally, by considering the PSNR results of all the despeckling methods on the pirate image with 0.05 and 0.1 noise variances, it is observed that the best and worst results belong to the proposed method and AMF. Moreover, for the houses image with 0.01 noise variance, it is observed that the proposed method with the PSNR value of 31.02 dB has the maximum value and the Kuan filter with the PSNR value of 26.31 dB denotes the minimum value. By considering the results obtained for boats, Lena and room images in the noise variance of 0.01, it is perceived that the NLM filter reached the best performance in term of PSNR value. After the NLM filter, the Wiener filter and the proposed method depict the second and third-best PSNR values in boats image. In the case of Lena image, in addition to NLM filter, the Wiener and wavelet filters have better performance than the proposed method. Finally, in the room image with the noise variance of 0.01, the proposed method with the PSNR value of 29.59 reached the second-rank after the NLM filter. Table 2 reveals the SSIM values resulting from the above-mentioned speckle noise reduction algorithms. The proposed method provides the best despeckling performance on all images for the noise variance of 0.05 and 0.1. For instance, in the noise variance of 0.05, it demonstrates the first-best performance on the

boats, cat, houses, Lena, room, and pirate images with the SSIM of 0.629, 0.836, 0.723, 0.643, 0.683, and 0.725. Additionally, the reached SSIM values of 0.557, 0.789, 0.650, 0.571, 0.603, and 0.654 from the boats, cat, houses, Lena, room, and pirate images prove the proposed methods' proficiency in the noise variance of 0.1. Based on the results, it has been observed that the Frost filter has slightly similar SSIM values to the proposed method. However, Frost, Wiener and NLM filter exhibit relatively larger SSIM values in the boats image with a 0.01 noise variance. According to Table 2, NLM, Wiener and Frost filter have the best performance in boats image with 0.045, 0.023 and 0.008 margin to the proposed method. Although in Lena image, in addition to NLM, Frost and Wiener filters, the wavelet filter also presents better performance than the proposed method in the noise variance of 0.01. In the case of room image, the NLM and the proposed filters with the PSNR values of 0.845 and 0.832 ranked first and second at speckle noise reduction.

In Fig. 5, the CoC values of our proposed method and all aforementioned despeckling methods applied on six images are plotted for different noise levels. For example, Fig. 5(b) represents the CoC values for the cat image. According to this figure, results depict the supremacy of our method compared to other despeckling algorithms. The CoC values of 0.994, 0.986, and 0.980 are recorded for the proposed method in the cases of 0.01, 0.05, and 0.1 noise variances, respectively. Results also revealed that after the suggested method, other approaches including Frost, Lee, and average filters, have the highest CoC values for 0.05 and 0.1 noise variances. In the noise variance of 0.01, Wiener, Frost, and wavelet filters reached the highest CoC values after the proposed method. Furthermore, the proposed method's comparison results for the pirate image are illustrated in Fig. 5(e). By comparing the methods in the noise variance of 0.01, it was observed that the proposed method with the CoC value of 0.987 has the best performance, followed by CoC values of 0.986, 0.986, 0.984, 0.982, 0.980, 0.974, 0.973, and 0.969 for NLM, Wiener, wavelet, Frost, Lee, average, AMF, and Kuan filters. It is noteworthy to mention that by considering Lena, room and boats' results, it was perceived that the NLM filter has the highest CoC values in the noise variance of 0.01. In these cases, the proposed method has the second-best performance, while in the higher noise variances, it ranked first in speckle noise suppression.

6-2- Experiments on Real US Images

In this section, six real US images of breast cancer [42] with the resolution of 512×512 pixels are used to assess the performance of the proposed method and the state-of-the-art despeckling methods, which are mentioned in Section 6.1. These images are shown in Fig. 6(a-f). They are obtained from http://onlinemedicalimages.com.

It is noteworthy to mention that since the noise variance is unknown in this case, we have to follow the blind case structure for the proposed method. Looking at the US images, it can be perceived that they have

been corrupted by the medium to high speckle noise. Therefore, the p value should be selected from the range of 2 to 4 corresponding to the medium SNR. In this case, the proposed method is performed by the p =2. Filtered images using the proposed method are exhibited in Fig. 6(e-h). In these figures, it is observed

that the proposed method depicts a strong ability of speckle noise suppression. In addition, it preserves the edges and details efficiently.

The ENL metric is used for quantitative evaluation of the despeckling performance of different methods from US images in the absence of reference images. ENL is a standard measurement metric which measures the despeckling capability of different methods in the homogeneous areas [36, 43]. It can be computed by [6]:

$$ENL = \left(\frac{\mu}{\sigma} \right)^2 . \tag{15}$$

In this equation, the mean and standard deviation of homogeneous regions are depicted by μ and σ. The higher values of ENL presents an excellent despeckling ability.

In this paper, two regions of interest (ROI) in each filtered US images have been selected [36]. ROI are selected from the homogeneous regions of the filtered images as stated in [6, 36, 43]. The resolution of ROI1 and ROI2 is 60×110 pixels, and 85×60 pixels. The selected ROIs in each filtered US images are depicted in Fig. 6(e-h). ENL is calculated in these regions, and the results are listed in Table 3.

As depicted in Table 3, among all despeckling approaches considered, the NLM filter has the lowest ENL value in all of

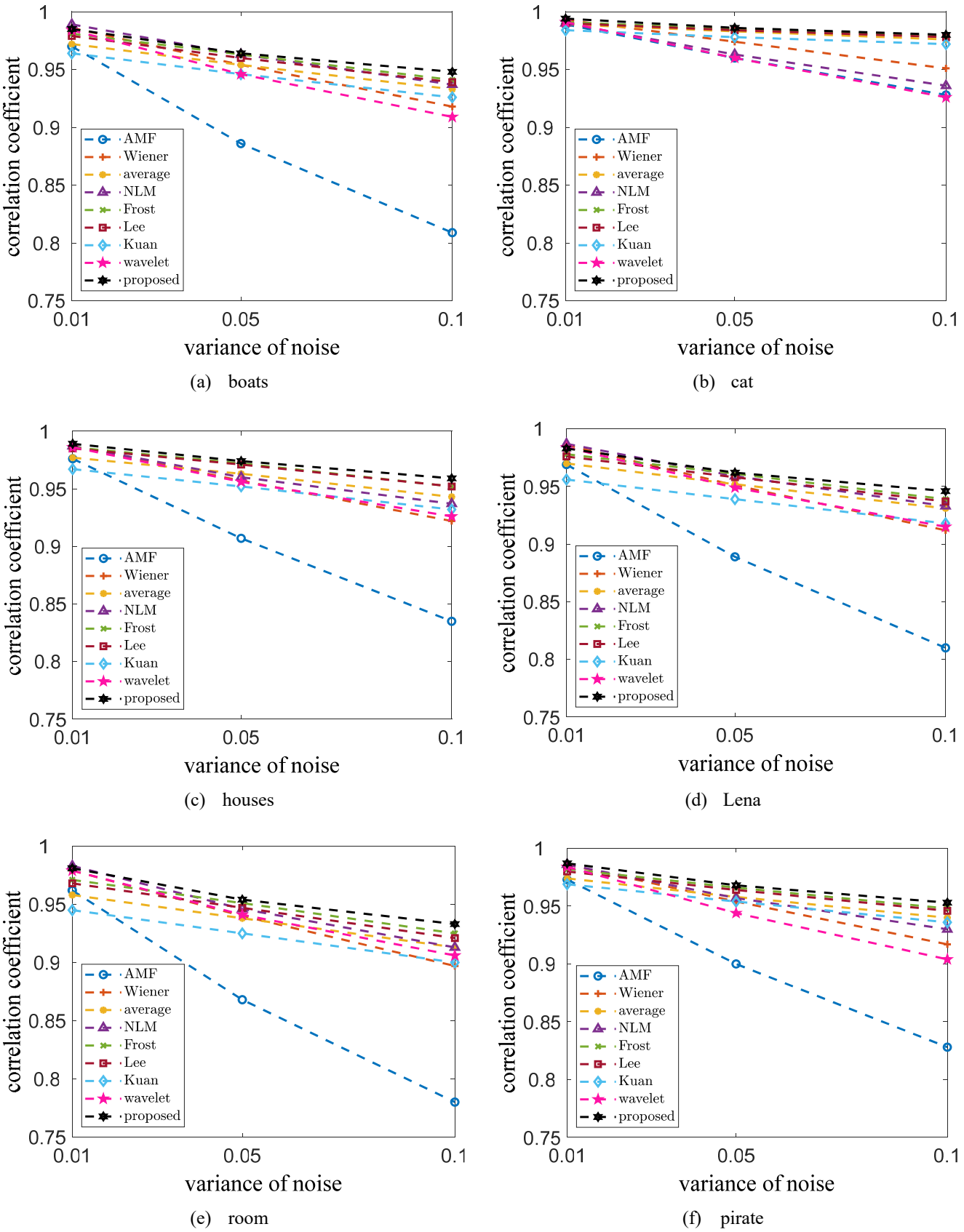

Fig. 5. Comparison of CoCs for different methods versus three noise variances (0.01, 0.05 and 0.1).

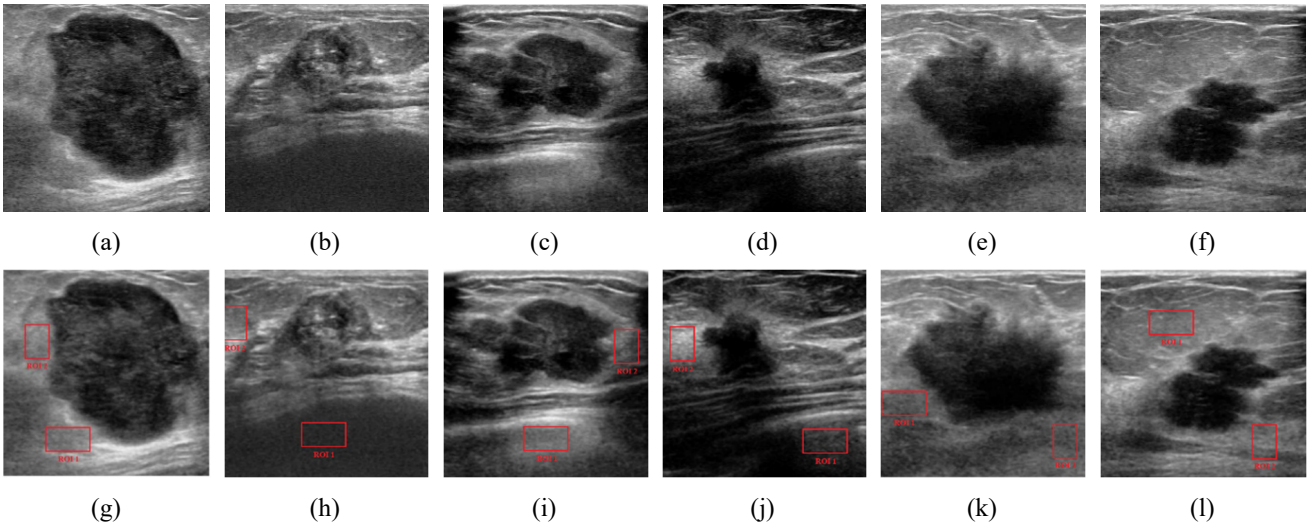

Fig. 6. (a-f) US images with resolution of 512×512 pixels. (g-l) Selected ROIs on the filtered US images.

Table 3. ENL obtained from the experiments on US images.

		AMF	Wiener	average	NLM	Frost	Lee	Kuan	wavelet	proposed
Patient 1	ROI 1	60.5	64.4	64.5	59.4	64.4	64.5	64.4	59.9	**69.2**
	ROI 2	81.4	88.5	88.7	79.5	88.7	88.7	88.7	80.2	**98.1**
Patient 2	ROI 1	63.6	83.7	83.7	57.8	82.0	83.7	82.2	60.4	**138.1**
	ROI 2	27.1	28.2	28.4	26.7	28.3	28.4	28.3	26.8	**29.0**
Patient 3	ROI 1	83.1	88.7	88.8	81.5	88.7	88.8	88.8	82.2	**96.5**
	ROI 2	13.8	14.4	14.4	13.7	14.4	14.4	14.4	13.7	**15.1**
Patient 4	ROI 1	12.1	13.2	13.3	11.9	13.2	13.3	13.3	12.0	**14.8**
	ROI 2	28.9	30.2	30.5	28.7	30.5	30.5	30.5	28.8	**32.6**
Patient 5	ROI 1	60.1	65.2	65.3	58.9	64.1	65.3	64.1	59.5	**72.7**
	ROI 2	62.9	70.0	70.1	61.4	70.0	70.1	70.1	62.0	**81.2**
Patient 6	ROI 1	118.1	133.2	133.3	113.9	130.6	133.3	130.7	115.4	**156.1**
	ROI 2	38.8	41.3	41.3	38.3	41.2	41.3	41.3	38.5	**45.0**

the ROI (US image 1 (ENL1=59.4, ENL2=79.5), US image 2 (ENL1=57.8, ENL2=26.7), US image 3 (ENL1=81.5, ENL2=13.7), US image 4 (ENL1=11.9, ENL2=28.7)), US image 5 (ENL1=58.9, ENL2=61.4)) and US image 6 (ENL1=113.9, ENL2=38.3)). By considering the ENL results related to patient 3, the best to worst despeckling methods are proposed method (ENL1=96.5, ENL2=15.1), Lee, Kuan, average (ENL1=88.8, ENL2=14.4), Wiener, Frost (ENL1=88.7, ENL2=14.4), AMF (ENL1=83.1, ENL2=13.8), wavelet (ENL1=82.2, ENL2=13.7) and NLM (ENL1=81.5, ENL2=13.7) filters. According to Table 3, the proposed method outperforms the existing approaches by reaching the highest ENL values. After the proposed method, Lee and average filters rank second in despeckling with the ENL values of ENL1=64.5 and ENL2=88.7 in the US image 1, ENL1=83.7 and ENL2=28.4 in the US image 2, ENL1=88.8 and ENL2=14.4 in the US image 3, ENL1=13.3 and ENL2=30.5 in the US image 4, ENL1=65.3 and ENL2=70.1 in the US image 5, and ENL1=133.3 and ENL2=41.3 in the US image 6. We have computed the enhancement percentage of the proposed method based on the first and second-best despeckling filters' ENL values. The proposed approach has 7.3%, 65%, 8.7%, 11.3%, 11.3%, and 17.1% ENL improvement compared to the second-best despeckling filter in the ROI1 of the US images 1, 2, 3, 4, 5 and 6. Additionally, this method was 10.6%, 2.1%, 4.9%, 6.9%, 15.9% and 9% better than the Lee and average filters in the ROI2 of the US images 1, 2, 3, 4, 5 and 6.

In conclusion, the results in terms of PSNR, SSIM, CoC, and ENL exhibit the proposed method's excellent speckle noise suppression capability. Additionally, the visual assessment verifies this superiority.

7.CONCLUSION

In this work, we introduced a novel approach to estimate 2D Gaussian filter variance to effectively eliminate the speckle noise. The entropy of optimum p-norm, which is calculated for the difference between the noisy and denoised images, was proposed as a criterion to obtain the appropriate variance of the filter. The p root of optimum variance value can be calculated by finding the point where the maximum derivative of differential entropy occurs. Through this procedure, an estimate of the norm order was also addressed. Simulation results confirm the superiority of the proposed method in terms of quantitative evaluation and image quality indexes.

REFERENCES

[1] M. Ambrosanio, B. Kanoun, F. Baselice, wKSR-NLM: An Ultrasound Despeckling Filter Based on Patch Ratio and Statistical Similarity, IEEE Access, 8 (2020) 150773-150783.

[2] H. Aetesam, S.K. Maji, Ultrasound Image Deconvolution adapted to Gaussian and Speckle Noise Statistics, in: 2020 7th International Conference on Signal Processing and Integrated Networks (SPIN), IEEE, 2020, pp. 1114-1119.

[3] W. Cui, M. Li, G. Gong, K. Lu, S. Sun, F. Dong, Guided trilateral filter and its application to ultrasound image despeckling, Biomedical Signal Processing and Control, 55 (2020) 101625.

[4] L.H. Breivik, S.R. Snare, E.N. Steen, A.H.S. Solberg, Real-time nonlocal means-based despeckling, IEEE transactions on ultrasonics, ferroelectrics, and frequency control, 64(6) (2017) 959-977.

[5] K. Mei, B. Hu, B. Fei, B. Qin, Phase asymmetry ultrasound despeckling with fractional anisotropic diffusion and total variation, IEEE Transactions on Image Processing, 29 (2019) 2845-2859.

[6] [6] F. Mei, D. Zhang, Y. Yang, Improved non-local self-similarity measures for effective speckle noise reduction in ultrasound images, Computer Methods and Programs in Biomedicine, 196 (2020) 105670.

[7] R. Lalchhanhima, D. Kandar, R. Chawngsangpuii, Single Look SAR Image Segmentation Using Local Entropy, Median Low-Pass Filter and Fuzzy Inference System, in: International Conference on Machine Learning, Image Processing, Network Security and Data Sciences, Springer, 2020, pp. 149-159.

[8] U. Erkan, S. Engınoğlu, D.N. Thanh, A recursive mean filter for image denoising, in: 2019 International Artificial Intelligence and Data Processing Symposium (IDAP), IEEE, 2019, pp. 1-5.

[9] S.I. Jabbar, C. Day, E. Chadwick, Automated reduction the speckle noise of the panoramic ultrasound images of Muscles and Tendons, in: Journal of Physics: Conference Series, IOP Publishing, 2020, pp. 012085.

[10] N. Bodaisingi, B. Narayanam, Techniques for de-noising of bio-medical images, (2018).

[11] M.H. Bibalan, H. Amindavar, Non-Gaussian amplitude PDF modeling of ultrasound images based on a novel generalized Cauchy-Rayleigh mixture, EURASIP Journal on Image and video Processing, 2016(1) (2016) 1-12.

[12] Y. Tounsi, M. Kumar, A. Nassim, F. Mendoza-Santoyo, O. Matoba, Speckle denoising by variant nonlocal means methods, Applied optics, 58(26) (2019) 7110-7120.

[13] D. Yin, Z. Gu, Y. Zhang, F. Gu, S. Nie, S. Feng, J. Ma, C. Yuan, Speckle noise reduction in coherent imaging based on deep learning without clean data, Optics and Lasers in Engineering, 133 (2020) 106151.

[14] S. Saravani, R. Shad, M. Ghaemi, Iterative adaptive Despeckling SAR image using anisotropic diffusion filter and Bayesian estimation denoising in wavelet domain, Multimedia Tools and Applications, 77(23) (2018) 31469-31486.

[15] F. Nar, SAR image despeckling using quadratic–linear approximated-norm, Electronics Letters, 54(6) (2018) 387-389.

[16] A. Gupta, V. Bhateja, A. Srivastava, A. Gupta, Suppression of speckle noise in ultrasound images using bilateral filter, in: Information and communication technology for intelligent systems, Springer, 2019, pp. 735-741.

[17] Z. Zhou, E.Y. Lam, C. Lee, Nonlocal means filtering based speckle removal utilizing the maximum a posteriori estimation and the total variation image prior, IEEE Access, 7 (2019) 99231-99243.

[18] W. Feng, H. Lei, Combination of geometric clustering and nonlocal means for SAR image despeckling, Electronics letters, 50(5) (2014) 395-396.

[19] D. Gupta, R. Rathi, S. Gupta, An Efficient Approach of Filtering for Noises on Images, in: 2018 4th International Conference on Computing Communication and Automation (ICCCA), IEEE, 2018, pp. 1-5.

[20] T. Tasnim, M.M.H. Shuvo, S. Hasan, Study of speckle noise reduction from ultrasound b-mode images using different filtering techniques, in: 2017 4th International Conference on Advances in Electrical Engineering (ICAEE), IEEE, 2017, pp. 229-234.

[21] Z. Hosseini, M.H. Bibalan, Speckle Noise Reduction Of Ultrasound Images Based On Neighbor Pixels Averaging, in: 2018 25th National and 3rd International Iranian Conference on Biomedical Engineering (ICBME), IEEE, 2018, pp. 1-6.

[22] P. Kalavathi, M. Abinaya, S. Boopathiraja, Removal of Speckle Noise in Ultrasound Images using Spatial Filters, in: National Conference on Computational Methods, Communication Techniques and Informatics, 2017, pp. 174-177.

[23] Z. Yu, W. Wang, C. Li, W. Liu, J. Yang, Speckle noise suppression in SAR images using a three-step algorithm, Sensors, 18(11) (2018) 3643.

[24] X. Fu, Y. Wang, L. Chen, Y. Dai, Quantum-inspired hybrid medical ultrasound images despeckling method, Electronics Letters, 51(4) (2015) 321-323.

[25] H. Seddik, A new family of Gaussian filters with adaptive lobe location and smoothing strength for efficient image restoration, EURASIP Journal on Advances in Signal Processing, 2014(1) (2014) 1-11.

[26] Y. Jin, W. Jiang, J. Shao, J. Lu, An improved image denoising model based on nonlocal means filter, Mathematical Problems in Engineering, 2018 (2018).

[27] D. Chan, J. Gambini, A.C. Frery, Speckle Noise Reduction In Sar Images Using Information Theory, in: 2020 IEEE Latin American GRSS & ISPRS Remote Sensing Conference (LAGIRS), IEEE, 2020, pp. 456-461.

[28] M. Gupta, A. Garg, An efficient technique for speckle noise reduction in ultrasound images, in: 2017 4th International Conference on Signal Processing and Integrated Networks (SPIN), IEEE, 2017, pp. 177-180.

[29] S.K. Kopparapu, M. Satish, Identifying optimal Gaussian filter for Gaussian noise removal, in: 2011 Third National Conference on Computer Vision, Pattern Recognition, Image Processing and Graphics, IEEE, 2011, pp. 126-129.

[30] E. Rifkah, A. Amer, Automated Gaussian filtering VIA Gaussian scale space and linear diffusion, in: 2012 Proceedings of the 20th European Signal Processing Conference (EUSIPCO), IEEE, 2012, pp. 1539-1542.

[31] Y. Zhang, Y. Lu, Z. Zhang, J. Wang, C. He, T. Wu, Noise reduction by Brillouin spectrum reassembly in Brillouin optical time domain sensors, Optics and Lasers in Engineering, 125 (2020) 105865.

[32] S. Yin, Y. Qian, M. Gong, Unsupervised hierarchical image segmentation through fuzzy entropy maximization, Pattern Recognition, 68 (2017) 245-259.

[33] J. Prakash, S. Mandal, D. Razansky, V. Ntziachristos, Maximum entropy based non-negative optoacoustic tomographic image reconstruction, IEEE Transactions on Biomedical Engineering, 66(9) (2019) 2604-2616.

[34] Y. Shen, Q. Liu, S. Lou, Y.-L. Hou, Wavelet-based total variation and nonlocal similarity model for image denoising, IEEE Signal Processing Letters, 24(6) (2017) 877-881.

[35] L. Fabbrini, M. Greco, M. Messina, G. Pinelli, Improved anisotropic diffusion filtering for SAR image despeckling, Electronics letters, 49(10) (2013) 672-674.

[36] H. Choi, J. Jeong, Speckle noise reduction technique for SAR images using statistical characteristics of speckle noise and discrete wavelet transform, Remote Sensing, 11(10) (2019) 1184.

[37] J.L. Mateo, A. Fernández-Caballero, Finding out general tendencies in speckle noise reduction in ultrasound images, Expert systems with applications, 36(4) (2009) 7786-7797.

[38] A.M. Molaei, M. Sedaaghi, H. Ebrahimnezhad, Steganography scheme based on Reed-Muller Code with improving payload and ability to Retrieval of Destroyed data for digital images, AUT Journal of Electrical Engineering, 49(1) (2017) 53-62.

[39] U. Sara, M. Akter, M.S. Uddin, Image quality assessment through FSIM, SSIM, MSE and PSNR—a comparative study, Journal of Computer and Communications, 7(3) (2019) 8-18.

[40] F. Yaghmaee, E. Kalatehjari, Reduced-Reference Image Quality Assessment based on saliency region extraction, AUT Journal of Electrical Engineering, 51(1) (2019) 83-92.

[41] S. Sahu, H.V. Singh, B. Kumar, A heavy-tailed levy distribution for despeckling ultrasound image, in: 2017 Fourth International Conference on Image Information Processing (ICIIP), IEEE, 2017, pp. 1-5.

[42]] A. Rodtook, K. Kirimasthong, W. Lohitvisate, S.S. Makhanov, Automatic initialization of active contours and level set method in ultrasound images of breast abnormalities, Pattern Recognition, 79 (2018) 172-182.

[43] F. Baselice, Ultrasound image despeckling based on statistical similarity, Ultrasound in medicine & biology, 43(9) (2017) 2065-2078.

HOW TO CITE THIS ARTICLE

Z.Hosseini, M.Hassannejad Bibalan, Entropy Based Parameter Estimation of 2D Gaussian Filter for Image Speckle Noise Removal, AUT J. Elec. Eng., 53(2) (2021) 189-200.

DOI: 10.22060/eej.2021.19374.5389